Editors' Suggestion

Searching for Coleman–de Luccia bubbles in AdS compactifications

Giuseppe Dibitetto[1,*] and Nicolò Petri[2,†]

[1]*Dipartimento di Fisica, Università di Roma "Tor Vergata" and Sezione INFN Roma 2, Via della ricerca scientifica 1, 00133 Roma, Italy*

[2]*Department of Physics, Ben-Gurion University of the Negev, Be'er-Sheva 84105, Israel*

(Received 16 January 2023; accepted 2 February 2023; published 27 February 2023)

Coleman–de Luccia transitions are spontaneous processes of nucleation of bubbles within metastable gravitational vacua including in their interior a true stable vacuum. From the perspective of lower-dimensional gauged supergravities obtained by truncating type II and M theory, these instantonic processes are represented by smooth domain walls featured by de Sitter foliations. These geometries must connect two different anti–de Sitter (AdS) vacua in such a way that the wall is defined by an interior and an exterior. We propose a first-order formulation for such radial flows and present two fully backreacted examples of gravitational instantons obtained through this technique, beyond the thin-wall approximation. In the first, we consider minimal 7D supergravity describing the truncation of M theory over a squashed four-sphere and admitting two AdS_7 vacua, one supersymmetric and the other not. Second, we apply the same strategy to 6D Romans supergravity obtained with consistent truncation of massive IIA supergravity. Also in this case we derive a de Sitter domain wall interpolating between the Brandhuber-Oz vacuum and the nonsupersymmetric AdS_6 vacuum of the theory.

DOI: 10.1103/PhysRevD.107.046020

I. INTRODUCTION

Ever since the very birth of string theory as a candidate UV complete description of gravitational interactions, it has passed a number of nontrivial theoretical tests that provide a compelling evidence for its UV consistency. These include crucial facts such as black hole microstate counting [1], as well as the AdS/CFT correspondence [2]. Moreover, a few preliminary investigations carried out in some controlled setups even seem to suggest that string theory might actually comprise the entirety of all field theory constructions that are consistent in the UV. This statement is usually referred to as the string universality principle [3,4].

However, all of the above features seem to crucially rely on supersymmetry as a protection mechanism, or at least one could say that we have only been able to draw concrete conclusions within supersymmetric settings. This may be due to the fact that the presence of supersymmetry often allows for analytic treatment and plays a crucial role in making things calculable. In this context, it should not sound surprising that the biggest challenge posed by the string theory paradigm is that of providing a satisfactory mechanism for spontaneous supersymmetry breaking. Needless to say, this is of utmost importance when it comes to connecting our UV consistent theory with a low-energy effective model possessing the desired phenomenological properties to describe the world we observe.

In the last two decades, the string universality principle has been addressed by adopting a complementary bottom-up approach, i.e., by trying to assess which seemingly consistent field theoretical constructions can actually be UV completed to fully consistent quantum theories. This way, one might think of coming up with a set of consistency criteria that a low-energy description must comply with in order for it to be related to string theory in an appropriate limit. This approach, also known as the string swampland program [5], has been developing in the last few years, in particular, and has delivered a lot of interesting connections among different desirable IR properties of a given model. We refer the reader to [6,7] for a nice review of the recent developments in this field.

The prototypical string swampland conjecture appeared back in the mid-2000s [8], where it is argued that a sensible quantum theory describing the interaction between gravity and gauge fields should always retain gravity as the weakest force in the game. The practical criterion proposed there is that there should always exist a microscopic particle in the spectrum, i.e., a particle whose mass is smaller than its charge in Planck units. The authors of [8] are able to relate

*giuseppe.dibitetto@roma2.infn.it
†petri@post.bgu.ac.il

Published by the American Physical Society under the terms of the Creative Commons Attribution 4.0 International license. Further distribution of this work must maintain attribution to the author(s) and the published article's title, journal citation, and DOI. Funded by SCOAP³.

this to the common lore that continuous global symmetries should not exist in quantum gravity.

It is worth noting that, contrary to microscopic particles predicted by the weak gravity conjecture (WGC), macroscopic particles always satisfy a Bogomol'nyi-Prasad-Sommerfield (BPS) bound instead, i.e., $M \geq QM_{\mathrm{Pl}}$. In particular, BPS states happen to saturate this inequality, thus being in some sense microscopic and macroscopic objects at the same time. Indeed, the presence of BPS states in the spectrum is protected by supersymmetry all the way from weak to strong coupling. This feature is at the basis of the stability arguments for supersymmetric configurations [9].

More recently, in [10], a stronger version of the WGC was proposed, according to which only BPS particles can saturate the BPS bound, this implying that in the absence of supersymmetry there must exist microscopic objects with mass strictly smaller than their charge. Note that, in the context of higher-dimensional gravitational theories, the aforementioned objects need not even be particles. These might be extended charged membranes, and their mass should be replaced by the tension. The authors of [10] infer the nonperturbative instability of nonsupersymmetric anti–de Sitter (AdS) vacua in string theory as a direct implication of this. Such a nonsupersymmetric d-dimensional vacuum would then be destroyed by spontaneous nucleation of charged microscopic $(d-2)$ membranes that eventually discharge the flux supporting the original vacuum.

It is worth stressing that this instability may result in the absence of a holographic conformal field theory (CFT) dual. From a gravitational viewpoint, this may be seen as a consequence of the fact that any local instability occurring somewhere in the bulk would take a finite global time to reach the boundary of AdS, where its dual CFT is supposed to live [11]. If one has the underlying brane picture in mind, what prevents taking the conformal limit in a nonsupersymmetric setting is the impossibility to pile up the branes into a stack, as they would feel a force repelling each other due to the WGC. As a consequence, checking nonperturbative stability of AdS vacua is crucial for their holographic interpretation to hold. However, this is, in general, not easy a task within the full stringy description of the given vacuum. We refer to [12] as an example where the proper stringy treatment has been illustrated.

On the other hand, nonperturbative decay processes such as gravitational tunneling events have been widely studied since the beginning of the 1980s [13,14] within the framework of semiclassical Euclidean path integrals in 4D gravity. The tunneling process between two classical vacua is seen as a bubble nucleation event for observers living in the false vacuum geometry. Enclosed within the bubble wall, there is the true vacuum geometry. Viable decay channels correspond to local extrema of the Euclidean action. In the thin shell limit, these are identified by junctions respecting the so-called Coleman–de Luccia (CdL) bound [13]. Going beyond the thin limit means being able to dynamically source the jumps in the fields across the aforementioned junction by employing extra scalar fields. This procedure generically results in a smooth interpolating geometry called a domain wall (DW).

DW solutions have been extensively explored in the context of lower-dimensional supergravity theories. In particular, when supersymmetry is preserved, these turn out to obey first-order flow equations determined by the corresponding Killing spinors. This often allows one to analytically determine the corresponding dynamical profiles. In this paper, we will show how positively curved DWs are directly related to the aforementioned CdL bubbles and are intrinsically nonsupersymmetric. Despite this, we will make use of the Hamilton-Jacobi (HJ) formalism in order to provide a first-order formulation thereof [15]. This will allow us to overcome the problem of sensitivity to the choice of initial data, which the second-order formulation suffers from.

Similar techniques were recently used in [16], where positively curved domain wall solutions connecting different AdS vacua were explicitly found. The setup there is a generic Einstein-scalar theory with the addition of a negative cosmological constant, though the explicit choices of scalar potentials are not directly linked to a specific higher-dimensional origin. Besides discussing in detail their interpretation on the gravity side as CdL bubbles, the authors of [16] also identify their holographic description to be a CFT on a cylinder $\mathbb{R} \times S^{d-1}$, rather than on flat space.

In our work, we want to take a further step and connect our lower-dimensional solutions to string and M theory. The crucial ingredient to achieve this will be the existence of consistent truncations [17]. To this end, we will apply the aforementioned technique to lower-dimensional supergravity models in dimension six and seven, which are known to arise from consistent truncations of massive type IIA supergravity [18] and 11D supergravity [19] on a (squashed) four-sphere, respectively. At this point, any lower-dimensional solution (including our CdL bubbles) have a natural higher-dimensional interpretation. A much harder task would then be that of understanding these bubbles as composite objects made out of fundamental stringy or M-theoretical building blocks, such as strings and membranes. For the moment, we will leave this out for future investigation.

The paper is organized as follows. In Sec. II, we briefly review the basics of CdL bubbles and their relation to the general classification of DWs by [20]. In Sec. III, we review the consistent truncation of 11D supergravity on a squashed S^4. Subsequently, within the truncated 7D supergravity theory, we present the numerical solution of interest describing a CdL instanton within the nonsupersymmetric AdS_7 vacuum of the theory. In Sec. IV, we apply the same machinery within Romans supergravity in 6D, which stems

from massive type IIA supergravity on S^4. In the Appendix, we present some general facts and introduce some notation concerning the HJ formalism.

II. COLEMAN–DE LUCCIA DECAYS AND DS DOMAIN WALLS

The process of gravitational tunneling can be seen as the spontaneous nucleation of a true vacuum bubble within a false vacuum geometry, and it can be studied within a semiclassical regime by Euclidean path integral techniques. This was done already in the early 1980s [13] by adopting the thin-wall approximation, where an infinitely thin bubble wall separates two different regions, each one characterized by a different value of the cosmological constant, say $\Lambda_\pm$. In [13], it was found that in 4D a critical value for the tension of the bubble wall (expressed in Planck units)

$$\sigma \overset{!}{\leq} \sigma_{\mathrm{CdL}} \equiv \frac{2}{\sqrt{3}}\left(-\sqrt{|\Lambda_+|}+\sqrt{|\Lambda_-|}\right), \tag{1}$$

is an upper bound in order for the Euclidean action to admit a local extremum. This is usually referred to as the Coleman–de Luccia bound. Later, in [14], it is shown that the mechanism of extremization for the Euclidean action can be physically understood as imposing energy conservation during the nucleation process. In this context, the CdL bound represents the allowed range of wall tensions admitting a finite bubble radius guaranteeing energy conservation. For a wall tension exactly saturating the CdL bound, the bubble radius becomes infinite, thus yielding a flat static wall rather than an actual bubble. For values larger than this critical value, no real bubble size turns out to be compatible with energy conservation. Once the Euclidean action is extremized at some finite value, the corresponding instanton configuration contributes to the decay rate of the vacuum through

$$\Gamma_{\mathrm{decay}} \sim e^{-S_E(\mathrm{instanton})}. \tag{2}$$

Back in Lorentzian signature, these instanton geometries correspond to DWs connecting two different vacuum solutions. Within the thin-wall approximation, these DWs are obtained by gluing two different maximally symmetric vacuum solutions with different values of the cosmological constant to each other, across a certain interface. Such DWs were studied and classified in [20]. The general form of the metric reads

$$ds^2_{d+1} = dr^2 + e^{2A(r)}L^2 ds^2_d, \tag{3}$$

where the metric for the d-dimensional slices ds^2_d is chosen to be maximally symmetric, and the asymptotic behavior of the warp factor A must be specified in such a way that the asymptotic geometries on the two sides of the wall are $(d+1)$-dimensional maximally symmetric vacua.[1] Let us now explore in detail all the possible features that fully characterize DW solutions.

A. Domain wall zoology

Once denoted by $\Lambda_\pm$ the cosmological constants on each side, and by κ the curvature parameter of the wall, solving the Einstein equations in the thin-wall limit turns out to be equivalent to solving the so-called Israel junction condition [21]. This essentially fixes the DW tension as to compensate for the jump in extrinsic curvature across the wall. As a result, the DW tension in Planck units[2] can be expressed as [20]

$$\sigma = \eta_+\sqrt{\frac{\kappa}{L^2}-\Lambda_+}+\eta_-\sqrt{\frac{\kappa}{L^2}-\Lambda_-}, \tag{4}$$

where $\eta_\pm \in \{\pm 1\}$ represent the orientations of the normal vector on the two sides of the wall. In particular, -1 indicates an exterior, while $+1$ indicates an interior.

In order then to fully characterize a DW, it turns out to be sufficient to specify its thin-wall data, i.e.,

(i) the signs of $\Lambda_\pm$ (0 allowed),
(ii) the DW curvature parameter $\kappa = 0, \pm 1$,
(iii) the signs of $\eta_\pm$.

The first choice selects the case of interest out of a list of six possibilities [20]: dS/dS, dS/Mkw, dS/AdS, Mkw/Mkw, Mkw/AdS, and AdS/AdS. It is worth noting that the first three involving dS space never admit the extreme limit, i.e., taking $L \to \infty$. This applies to some extent to Mkw/Mkw DWs as well, as extremal ones have vanishing tension. The remaining two choices, which do admit an extreme limit, were studied in detail in [22] in the supersymmetric BPS case, where extremality is guaranteed. There the analysis is performed even beyond thin wall, thanks to first-order flow equations implied by the existence of Killing spinors.

Of particular interest to our scope is the case of AdS/AdS DWs, since we will see that, under certain circumstances, they will precisely describe CdL bubbles. In [22], the key feature distinguishing different AdS/AdS DWs is whether or not the superpotential W vanishes somewhere along the flow. This identifies a nonmonotonic flow (dubbed type II), or rather a monotic one (dubbed type III), respectively. In the thin-wall limit, this is directly related to the choice of orientation ($\eta_\pm$) on the two sides, determining if the wall

[1]Note that the constant L just represents some reference length that makes ds^2_d dimensionless. For (A)dS, it just represents the (A)dS radius, while in Minkowski it is completely irrelevant, as it can reabsorbed into a redefinition of the spacetime coordinates.

[2]We also drop here $\mathcal{O}(1)$ constant factors that are not crucial for the sake of our conceptual treatment. Besides, these would make it harder to provide a general discussion in arbitrary d, as they explicitly depend on the number of spacetime dimensions.

has two insides (I/I), two outsides (O/O), or an inside and an outside (I/O).

If we now compare the CdL critical tension in (1) with (4), we immediately see that they exactly coincide for $\kappa = 0$ and $\eta_+ = -1$, $\eta_- = +1$, i.e., an extremal (flat) I/O DW. For I/O walls with general κ, the tension reads

$$\sigma = \sqrt{\frac{\kappa}{L^2} - \Lambda_-} - \sqrt{\frac{\kappa}{L^2} - \Lambda_+} \to \begin{cases} > \sigma_{\mathrm{CdL}}, & \kappa = -1, \\ = \sigma_{\mathrm{CdL}}, & \kappa = 0, \\ < \sigma_{\mathrm{CdL}}, & \kappa = +1. \end{cases} \tag{5}$$

This implies that actual gravitational instantons such as CdL bubbles are represented by I/O DWs with dS slices [23].

On the other hand, for a $(-1,-1)$ choice of orientation (corresponding with a wall with two outsides), one has an object with negative tension. The effect of placing this wall at some finite r in DW coordinates is that of cutting out a portion of infinite volume from spacetime, thus rendering the total effective volume finite. This is exactly a Randall-Sundrum (RS) brane, which was used in [24] in order to produce an effective 4D braneworld within AdS_5 in such a way that 4D gravity be localized on the brane. While locally such a spacetime looks like AdS on both sides, globally it has no boundaries, since they have been removed on both sides.

Finally, if one considers the situation with two insides, the tension overcomes the CdL bound. This means that such an object would not be spontaneously created, but it is rather an exotic extended source that formally solves the junction condition. The local geometric structure still looks like AdS on both sides, but globally, unlike the RS brane, it has two boundaries placed at finite proper distance. In this sense, we qualify this object as a wormhole. The physically inequivalent AdS/AdS positively curved DWs are illustrated in Table I.

In the following sections, we will consider two examples of lower-dimensional supergravity theories with a known higher-dimensional origin and we will show how to construct I/O AdS/AdS positively curved DWs. As we have just been arguing, these correspond with CdL bubbles describing nonperturbative decays of an AdS false vacuum into an AdS true one. The technique we will make use of is the HJ formalism, which allows us to recast the original second-order differential problem into a first-order one. Thanks to this, we will get rid of the fine-tuning problem related to the choice of initial data, as it will be completely hidden into the correct choice of HJ generating functional. Upon numerical integration, we will obtain the desired solutions.

TABLE I. The inequivalent AdS/AdS spherical ($\kappa = +1$) domain walls. CdL bubbles are positively curved DWs with an inside and an outside. The remaining two situations, corresponding to exotic objects such as wormholes and RS branes, do not create spontaneously.

(η_-, η_+)	Orientation	Tension	Physical interpretation
$(+1,+1)$	I/I	$\sigma > \sigma_{\mathrm{CdL}}$	Wormhole
$(+1,-1)$	I/O	$0 < \sigma < \sigma_{\mathrm{CdL}}$	CdL bubble
$(-1,-1)$	O/O	$\sigma < 0$	RS brane

III. BUBBLE GEOMETRIES IN M THEORY

In this section, we derive a smooth bubble geometry connecting two different AdS_7 vacua, one supersymmetric and the other not. Our framework will be $\mathcal{N} = 1$ 7D supergravity obtained by truncating M theory on a squashed four-sphere using the compactification formulas of [19]. Our aim is to consider domain walls driven by one single scalar field and featured by a dS_6 slicing.

For such geometries, we construct the quantities needed in order to cast the second-order problem of the equations of motion into a first-order one, supplemented with one single extra partial differential equation (PDE), the Hamilton-Jacobi equation. The HJ formulation of classical systems, summarized in the Appendix, allows us to formulate the problem of finding the dynamics of the aforementioned domain walls in terms of a set of first-order ordinary differential equations (ODEs) whose solutions turn out to automatically satisfy the field equations.

The key of this procedure is finding the fake superpotential (the HJ generating functional) solving the Hamilton-Jacobi equation and defining the first-order system. In this section, we discuss various strategies to solve this problem for domain walls interpolating between the two AdS_7 vacua of the theory. Finally, we obtain an explicit numerical solution for this fake superpotential using a perturbative method whose efficiency perfectly suits this particular situation. Once we obtain the solution for the fake superpotential, we derive the radial flow of the interpolating domain wall.

A. Supergravity setup and AdS_7 vacua

It is well known that M theory can be consistently reduced over four-spheres (see, e.g., [19,25,26]). In this section, we are interested in the minimal truncation of 11D supergravity, namely, the truncation retaining only the 7D fields belonging to the supergravity multiplet (i.e., no matter couplings). The compactification reproducing such a theory is a warped compactification over a squashed S^4 and it has been worked out in [19]. Apart from the 7D gravitational field, this dimensional reduction yields one real scalar field X, three SU(2) vectors A^i, and a 3-form $B_{(3)}$ [27].

For the aim of this paper, we can focus on the case where the vectors and the 3-form are vanishing. The 11D truncation ansatz takes then the simplified form [19]

$$
\begin{aligned}
ds_{11}^2 &= \Delta^{1/3} ds_7^2 + 2g^{-2}\Delta^{-2/3} ds_4^2, \\
ds_4^2 &= \Delta X^3 d\xi^2 + X^{-1} c^2 ds_{S^3}^2, \quad \text{with} \\
\Delta &= X c^2 + X^{-4} s^2,
\end{aligned} \tag{6}
$$

where, for simplicity of notation, $s = \sin\xi$ and $c = \cos\xi$. With the assumption of vanishing 7D form fields, the 11D 4-form boils down to [19]

$$
\begin{aligned}
G_{(4)} = &-2\sqrt{2} g^{-3} c^3 \Delta^{-2} (X^{-8} s^2 - 2X^2 c^2 \\
&+ 3X^{-3} c^2 - 4X^{-3}) d\xi \wedge \mathrm{vol}_{S^3} \\
&- 10\sqrt{2} g^{-3} \Delta^{-2} X^{-4} c^4 s dX \wedge \mathrm{vol}_{S^3}.
\end{aligned} \tag{7}
$$

The above truncation defines a gauged supergravity with $\mathbb{R}^+ \times \mathrm{SO}(3)$ symmetry and features two gauge couplings g and h. The first is associated with the R-symmetry $\mathrm{SU}(2)_R$ group that is gauged in this theory and the second is a Stückelberg mass for the 3-form. The scalar potential for the scalar X has the form

$$
V = 2h^2 X^{-8} - 16h^2 X^{-3} - 16h^2 X^2, \tag{8}
$$

where the explicit truncation of [19] has fixed $g = 2\sqrt{2}h$. The Lagrangian of this theory is thus given by

$$
\sqrt{-g}^{-1} \mathcal{L} = R - 5X^{-2} \partial_\mu X \partial^\mu X - V, \tag{9}
$$

leading to the equations of motion

$$
\begin{aligned}
&R_{\mu\nu} - 5X^{-2} \partial_\mu X \partial_\nu X - \frac{1}{5} V g_{\mu\nu} = 0, \\
&\partial_\mu (\sqrt{-g} X^{-1} g^{\mu\nu} \partial_\nu X) - \frac{\sqrt{-g}}{10} X \partial_X V = 0.
\end{aligned} \tag{10}
$$

This theory has two AdS_7 vacua, a supersymmetric (SUSY) and a nonsupersymmetric one. Let us now consider them separately.

1. SUSY AdS_7 vacuum: $X = 1$

This vacuum is preserving 16 real supercharges and it is realized for $X = 1$. The 11D background takes the form of a direct product of AdS_7 and a round S^4,

$$
\begin{aligned}
ds_{11}^2 &= ds_{\mathrm{AdS}_7}^2 + 2g^{-2} ds_{S^4}^2, \\
G_{(4)} &= 6\sqrt{2} g^{-3} c^3 d\xi \wedge \mathrm{vol}_{S^3},
\end{aligned} \tag{11}
$$

with the radius of AdS_7 given by $L_{\mathrm{SUSY}} = 2\sqrt{2} g^{-1} = h^{-1}$. The brane interpretation of the above solution is clear. In fact, it can be viewed as the Freund-Rubin vacuum associated with the near-horizon geometry of a stack of M5 branes.[3] Alternatively one can also view (11) as the half-supersymmetric 11D vacuum arising from M5 branes on an A-type singularity.

2. Non-SUSY AdS_7 vacuum: $X = 2^{-1/5}$

A nonsupersymmetric AdS_7 vacuum can be obtained by setting $X = 2^{-1/5}$. In this case, the geometry is warped

$$
\begin{aligned}
ds_{11}^2 = &\, 2^{-1/15} (2 - c^2)^{1/3} [ds_{\mathrm{AdS}_7}^2 + 2^{2/5} g^{-2} d\xi^2 \\
&+ 2^{7/5} g^{-2} (2 - c^2)^{-1} c^2 ds_{S^3}^2], \\
G_{(4)} = &\, 8\sqrt{2} g^{-3} c^3 (2 - c^2)^{-2} d\xi \wedge \mathrm{vol}_{S^3},
\end{aligned} \tag{12}
$$

with the radius of AdS_7 given by $L_{\mathrm{SU/SY}} = 2^{7/10}\sqrt{3} g^{-1} = \frac{\sqrt{3}}{2^{4/5}} h^{-1}$. Unlike the supersymmetric case, the brane interpretation of this vacuum is not clear as well as its derivation as near-horizon limit of some 11D brane solution.

B. First-order formulation for dS_6 domain walls

Let us now take the 7D theory (9) as the operative framework and study domain walls of the following type:

$$
\begin{aligned}
ds_7^2 &= e^{2A(r)} L^2 ds_{\mathrm{dS}_6}^2 + dr^2, \\
X &= X(r).
\end{aligned} \tag{13}
$$

As it is manifest, the worldvolume of these domain walls is curved by a dS_6 space described by the element $ds_{\mathrm{dS}_6}^2$ with radius L. The two functions $A(r)$ and $X(r)$ specify the (11D) geometry. This class of backgrounds is what we need in order to study an expanding bubble within a given vacuum. Of course also some global aspects are crucial in order to describe gravitational instantons and the false vacuum decay [28]. At the current stage of analysis, we may say that the search of such domain walls connected to AdS_7 vacua implies a particular choice of boundary conditions on the vacuum geometry at infinity, namely, foliating the vacua with dS. This parametrization is, in fact, the one in which the topology of an expanding bubble is manifest. The field equations (10) split into two second-order nonlinear ODEs for A and X,

$$
\begin{aligned}
&A'' + 6A'^2 - \frac{5e^{-2A}}{L^2} + \frac{1}{5} V = 0, \\
&X'' + 6A'X' - \frac{X'^2}{X^2} - \frac{1}{10} X^2 \partial_X V = 0,
\end{aligned} \tag{14}
$$

and a first-order differential constraint

[3] This maximally supersymmetric interpretation appears by considering this solution within the maximal SO(5) gauged theory. There a SUSY enhancement to 32 supercharges becomes manifest.

$$30A'^2 - \frac{5X'^2}{X^2} - \frac{30e^{-2A}}{L^2} + V = 0, \tag{15}$$

where $'$ denotes the derivative with respect to r. The condition (15) is the analog of the first Friedman equation (for real time cosmology) and is usually called the "Hamiltonian constraint" in this context. This condition must be dynamically satisfied by any solution of (14). The vacuum geometry can be obtained by choosing

$$A = \log\left(\sinh\left(\frac{r}{L}\right)\right), \tag{16}$$

and imposing $X = 1$ and $L_{\mathrm{SUSY}} = h^{-1}$ or $X = 2^{-1/5}$ and $L_{\mathrm{SU/SY}} = \frac{\sqrt{3}}{2^{4/5}h}$, respectively, for SUSY and non-SUSY cases discussed in Sec. III A.

Following the general discussion of the Appendix, we can look at the second-order problem (14) and (15) as a classical constrained system with dynamical variables A and X. Our aim is to recast the second-order problem into a first-order one by using the standard Hamilton-Jacobi formulation of classical dynamics. First of all, we point out that the second-order equations (14) can be obtained from the effective Lagrangian,

$$L_{\mathrm{eff}} = 30e^{6A}A'^2 - 5e^{6A}\frac{X'^2}{X^2} + \frac{30e^{4A}}{L^2} - e^{6A}V. \tag{17}$$

From this expression, we can extract the corresponding Hamiltonian by introducing the conjugate momenta $\pi_A = 60e^{6A}A'$ and $\pi_X = -10e^{6A}X^{-2}X'$ following the general expression (A2). Taking the Legendre transformation of (17) leads to the Hamiltonian

$$H_{\mathrm{eff}} = \frac{1}{120}e^{-6A}\pi_A^2 - \frac{1}{20}e^{-6A}X^2\pi_X^2 - \frac{30e^{4A}}{L^2} + e^{6A}V. \tag{18}$$

We can now introduce the fake superpotential $F = F(A, X)$ associated with the system (14) as the real function such that $\pi_A = \partial_A F$ and $\pi_X = \partial_X F$ satisfying the Hamilton-Jacobi equation

$$\frac{1}{120}e^{-6A}(\partial_A F)^2 - \frac{1}{20}e^{-6A}X^2(\partial_X F)^2 - \frac{30e^{4A}}{L^2} + e^{6A}V = 0, \tag{19}$$

where the constant E appearing in the general expression (A3) must be zero in order to satisfy the Hamiltonian constraint (15). We thus reduced the constrained the system of ODEs (14) and (15) to a single PDE that has to be satisfied by a suitable solution for the superpotential F. The radial dependence of the functions describing the domain walls (13) can be thus obtained by specifying the first-order constraints (A5) to our particular case, namely,

$$A' = \frac{1}{60}e^{-6A}\partial_A F \quad \text{and} \quad X' = -\frac{1}{10}e^{-6A}X^2\partial_X F. \tag{20}$$

As explained in the Appendix, the solutions of the above first-order equations automatically solve also the equations of motion, since imposing the conditions (20) is equivalent to extremizing the action (17).

C. Strategies of integration

Let us consider domain wall geometries of type (13) interpolating between two different AdS_7 vacua (16), namely, smooth solutions that, on one side, asymptotically reproduce the supersymmetric vacuum with $X = 1$ and on the other side the nonsupersymmetric one with $X = 2^{-1/5}$. In the last section, we showed how to cast the second-order problem of the equations of motion (14) in terms of a single PDE (19) for a superpotential $F(A, X)$. We want now to discuss possible strategies in solving the dynamics for this particular domain wall geometry.

The presence of the de Sitter foliation and our particular requirement on the asymptotic behavior make the search for explicit solutions for the superpotential a hard task. In fact, the contribution to the stress-energy tensor associated with the curvature of the dS_6 foliation does not allow one to formulate a separable ansatz for $F(A, X)$ and this forces us to approach the problem with numerical methods. This can be clearly seen by looking at the Hamilton-Jacobi equation (19),

$$\frac{1}{120}e^{-6A}(\partial_A F)^2 - \frac{1}{20}e^{-6A}X^2(\partial_X F)^2 + V_{\mathrm{eff}} = 0, \tag{21}$$

where we introduced the "effective" potential,

$$V_{\mathrm{eff}} = -\frac{30e^{4A}}{L^2} + e^{6A}V. \tag{22}$$

The first term in (22) is associated with the curvature of the dS_6 slicing and it does not allow one to separate the variables.[4]

In addition to this, the requirement of having different AdS_7 vacua in the two asymptotic regions does not mean that we can treat them as equivalent initial conditions for our integration. This can be seen by trying to perform a direct numerical integration of second-order equations of motion (14) by starting from a linearized expansion of the supersymmetric vacuum. Such integrations generically produce singular behaviors (connected with M5 sources) at the other end of the flow. From these attempts, it is

[4]In the flat limit $L \to \infty$, the dS_6 foliation can be substituted by 6D Minkowski spacetime. In this case, the superpotential takes the separable form $F = 4e^{6A}f(X)$ with $f = -\frac{h}{2}(X^{-4} + 4X)$ such that $V = -\frac{4}{5}(6f^2 - X^2\partial_X f^2)$.

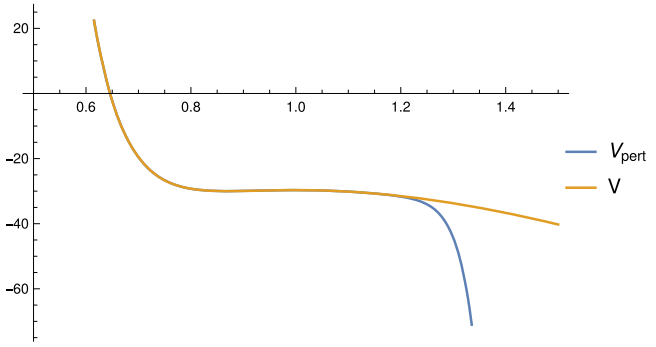

FIG. 1. The comparison between the scalar potential $V(X)$ written in (8) and its expansion at 15th order around the non-SUSY critical point $X = 2^{-1/5} \simeq 0.87$. For values of X between the two critical points $X \in [2^{-1/5}, 1]$, the scalar potential is well approximated by its expansion. The plot is given for $h = 2\sqrt{2}g = 1$.

manifest that the particular solution for A and X converging to the non-SUSY vacuum is determined by a set of initial parameters constituting a null measure set within the parameter space describing the linearized expansion around the SUSY vacuum. This can be rephrased by observing that the SUSY vacuum plays the role of an attractor point in the space of solutions (just like an M5 singularity does), while the non-SUSY one does not.

Given all of the above, we are led to approach the problem of integrating the Hamilton-Jacobi equation (21) by starting from a perturbative expansion of the fake superpotential $F(A, X)$ around the non-SUSY vacuum, namely, the point $X = 2^{-1/5}$ in the moduli space. The idea is to apply the perturbative method discussed in [29][5] to this particular situation and to solve order-by-order the perturbative tower of ODEs reproduced by the Hamilton-Jacobi equation when the superpotential is expanded around the non-SUSY vacuum. As it was pointed out in [29], in the case of domain walls with a curved worldvolume, the coefficients of the aforementioned expansion must depend on the warp factor of the metric A; this constitutes the main complication with respect to the case of domain walls with a flat slicing.

This procedure turns out to perfectly suit the current situation and we can test its effectiveness by comparing the 7D scalar potential $V(X)$ written in (8) with its Taylor expansion $V_{\text{pert}}(X)$ around the non-SUSY vacuum $X = 2^{-1/5}$ as in Fig. 1. For values of X included within the two extrema $X \in [2^{-1/5}, 1]$, at sufficiently high order, the scalar potential nicely coincides with its perturbative expansion, up to a great level of accuracy.

D. The interpolating solution

Since we are going to solve the Hamilton-Jacobi equation (21) with a perturbative expansion of the fake superpotential, we need to specify boundary conditions for F (or, more precisely, on its derivatives) that can be used to generate the initial conditions for the integration at each order. Such boundary data can be obtained by solving the Hamilton-Jacobi equation (21) for small values of the radius L. This regime is featured by a dominant contribution of the dS_6 curvature in the effective potential (22). In particular, one can verify that the expression

$$F_\infty = \frac{12}{L} e^{5A} - \frac{L}{7} e^{7A} V \tag{23}$$

solves the equation (21) up to $O(L^2)$ as $L \ll \ell_{\text{AdS}}$. As confirmed by the plot of Fig. 1, we can thus substitute V by its Taylor expansion V_{pert} around the point $X = 2^{-1/5}$ provided that the expansion be sufficiently large to reproduce a good matching of the curves in the interval $X \in [2^{-1/5}, 1]$. In this way, we can produce a set of initial conditions at each order in the expansion.

We can now write a perturbative ansatz of the form[6]

$$F(A, X) = 4 \sum_{k=0}^{\infty} F^{(k)}(A) \frac{(X - 2^{-1/5})^k}{k!}, \tag{24}$$

where the coefficients $F^{(k)}$ crucially depend on A [29] in order to take into account the nonseparability of the effective potential (22). The Hamilton-Jacobi equation (21) thus reproduces at $X = 2^{-1/5}$ a set of ODEs for the coefficients $F^{(k)}(A)$, each for any order in k. First of all, we observe that we need to impose that $F^{(1)}(A) = 0$ in order to keep each perturbative order decoupled. The zeroth-order equation takes the form

$$\frac{2}{15} e^{-6A} (\dot{F}^{(0)})^2 - \frac{30 e^{4A}}{L^2} - \frac{30 e^{6A}}{L^2} = 0, \tag{25}$$

where we denoted with $\cdot$ the derivative with respect to A and we expressed the scalar potential in terms of the radius of non-SUSY vacuum through the relation $h = \frac{2^{4/5}}{\sqrt{3}} L$ derived in (12). This equation can be solved exactly,

$$F^{(0)}(A) = \frac{5}{16L} e^A \sqrt{1 + e^{2A}} (-3 + 2e^{2A} + 8e^{4A}) + \frac{15}{16L} \operatorname{arcsinh}(e^A). \tag{26}$$

The subsequent step is to determine $F^{(2)}(A)$ by integrating the ODE appearing at order $k = 2$ with $F^{(0)}(A)$ given

[5]The perturbative method discussed in this reference further extends the one presented in [30].

[6]The factor of 4 is needed to reproduce the flat limit given by large values of L.

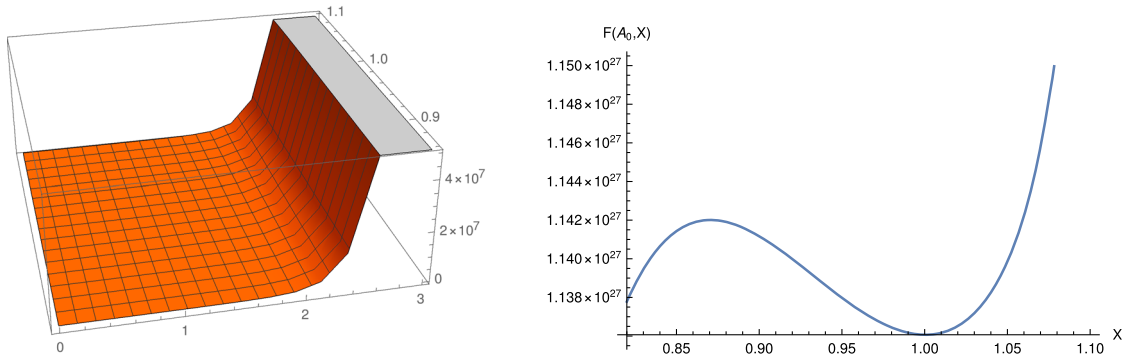

FIG. 2. The profile of the fake superpotential $F(A, X)$ obtained by iterating the perturbative integrations up to order $k = 15$. The 3D plot describes the full solution in the intervals $A \in [0, 3]$ and $X \in [0.86, 1.1]$. On the right side, the same function is plotted for $A_0 = 10$. Even if the variation of F is tiny, we observe an interpolating profile between the two AdS_7 vacua, respectively, located at $X = 2^{-1/5} \simeq 0.87$ and $X = 1$. The plots are given for $L = 1$.

in (26). This is a nonlinear ODE and it can be integrated numerically. Once this equation is solved (with a suitable initial condition that we specify below), each perturbative order in k can be solved iteratively in terms of the previous ones, since each of these equations turns out to be linear in $F^{(k)}(A)$. At each order in $k \geq 2$ we thus perform a numerical integration evaluating the $(k-1)$th solution of the previous step in the kth ODE for $F^{(k)}(A)$. As initial conditions, we choose

$$F^{(k)} = 4^{-1}\partial_X^k F_\infty^{(k)}|_{X=2^{-1/5}}, \tag{27}$$

where $F_\infty^{(k)}$ is given by (23) written in terms of the Taylor expansion of the scalar potential V at the kth order. Iterating the numerical integrations up to order $k = 15$, we obtain the solution plotted in Fig. 2. The relevant behavior can be observed in the plot on the right side where an interpolating behavior of F between the two vacua is manifest. This is the key property allowing the existence of interpolating domain walls. Given the numerical solution for the superpotential, we can finally integrate the first-order equations (20). For the sake of clarity, we rewrite them here as

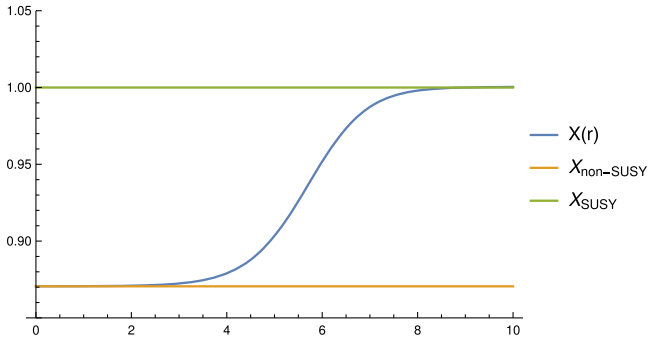

FIG. 3. The radial profile for the scalar X in the dS_6-sliced domain wall in comparison with those of the two AdS_7 vacua.

$$A' = \frac{1}{60}e^{-6A}\partial_A F \quad \text{and} \quad X' = -\frac{1}{10}e^{-6A}X^2\partial_X F. \tag{28}$$

We perform the numerical shooting using as initial value the non-SUSY vacuum placed at $r = 0$. The result is plotted in Fig. 3. We thus obtained a domain wall solution interpolating between the nonsupersymmetric and supersymmetric AdS_7 vacua.

IV. BUBBLE GEOMETRIES IN MASSIVE IIA

In this section, we apply the same strategy of Sec. III to the case of smooth dS_5 domain walls in massive IIA supergravity. In analogy to dS_6 bubbles in M theory, we will work within the consistent truncation of massive IIA supergravity on a squashed four-sphere constructed in [18]. This truncation reproduces a very similar framework to the 7D supergravity used in Sec. III, especially if one considers only the scalar sector. In fact, the lower-dimensional theory is the minimal incarnation of half-maximal gauged supergravity in 6D and admits two AdS_6 vacua associated with two different values of a single scalar field. In analogy with the 7D case, one vacuum is supersymmetric, while the other is not.

In this section, we will adopt the Hamilton-Jacobi formulation of classical dynamical systems in this 6D setup with the purpose of searching for smooth dS_5 bubbles connecting the above two different vacua. To this aim, we will apply the perturbative technique of Sec. III D to this particular framework.

A. Romans supergravity

Let us recall the main features of the consistent truncation of massive IIA supergravity constructed in [18]. This is a warped compactification defined by an internal squashed four-sphere and retaining only the fields belonging to the 6D supergravity multiplet without any matter multiplet. The isometry group is $\mathbb{R}^+ \times SO(4)$ and preserves 16 real

supercharges, namely, it is $\mathcal{N}=(1,1)$ theory in 6D. In addition to 6D gravity, the field content is given by one real scalar field X, three SU(2) vectors A^i, one Abelian vector A^0, and a 2-form $B_{(2)}$. This 6D gauged supergravity is usually called Romans supergravity [31]. We are interested in the case where all the vectors and the 2-form are vanishing. The ansatz for the metric and dilaton takes the form [18]

$$\begin{aligned} ds_{10}^2 &= X^{-1/2}\Delta^{1/2}s^{-1/3}[ds_6^2 + 2g^{-2}X^2 ds_4^2], \\ ds_4^2 &= d\xi^2 + \Delta^{-1}X^{-3}c^2 ds_{S^3}^2, \quad \text{with} \\ \Delta &= Xc^2 + X^{-3}s^2, \\ e^{\Phi} &= s^{-5/6}\Delta^{1/4}X^{-5/4}, \end{aligned} \tag{29}$$

and $s=\sin\xi$ and $c=\cos\xi$. After imposing that the vectors and the 2-form are vanishing, only the 4-form flux and the Romans mass $F_{(0)}=m$ survive, namely [18],

$$\begin{aligned} F_{(4)} = &-\frac{4\sqrt{2}}{3}g^{-3}\Delta^{-2}(X^{-6}s^2 - 3X^2c^2 \\ &+ 4X^{-2}c^2 - 6X^{-2})s^{1/3}c^3 d\xi\wedge \mathrm{vol}_{S^3} \\ &- 8\sqrt{2}g^{-3}\Delta^{-2}X^{-3}s^{4/3}c^4 dX\wedge \mathrm{vol}_{S^3}. \end{aligned} \tag{30}$$

The deformations of the 6D theory produced by this truncation are defined by two embedding tensor parameters, g and m. As in the 7D case, the first one is associated with the gauged R-symmetry group $\mathrm{SU}(2)_R$ and the second is a Stückelberg mass for the 2-form. The scalar potential has the form [18,31]

$$V = m^2X^{-6} - 12m^2X^{-2} - 9m^2X^2, \tag{31}$$

where we fixed $g=\frac{3m}{\sqrt{2}}$ as required by the truncation ansatz of [18]. The 6D Lagrangian has the form

$$\sqrt{-g}^{-1}\mathcal{L} = R - 4X^{-2}\partial_\mu X\partial^\mu X - V. \tag{32}$$

By taking the variation with respect to the metric and the scalar X one can easily obtain the equations of motion,

$$\begin{aligned} R_{\mu\nu} - 4X^{-2}\partial_\mu X\partial_\nu X - \frac{1}{4}Vg_{\mu\nu} = 0, \\ \partial_\mu(\sqrt{-g}X^{-1}g^{\mu\nu}\partial_\nu X) - \frac{\sqrt{-g}}{8}X\partial_X V = 0. \end{aligned} \tag{33}$$

This theory admits two different AdS_6 vacua, one supersymmetric and one not. Let us now consider them separately as in the case of 7D supergravity studied in Sec. III.

1. SUSY AdS_6 vacuum: $X=1$

This is the Brandhuber and Oz vacuum describing the near-horizon geometry of the D4-D8 branes [32]. It is realized for $X=1$ and preserves 16 real supercharges. The 10D geometry is defined by a warped product of AdS_6 with a four-sphere[7] S^4,

$$\begin{aligned} ds_{10}^2 &= s^{-1/3}[ds_{\mathrm{AdS}_6}^2 + 2g^{-2}ds_{S^4}^2], \\ e^{\Phi} &= s^{-5/6}, \\ F_{(4)} &= \frac{20\sqrt{2}}{3}g^{-3}s^{1/3}c^3 d\xi\wedge \mathrm{vol}_{S^3}, \end{aligned} \tag{34}$$

with the radius of AdS_6 given by $L_{\mathrm{SUSY}}=\frac{3}{\sqrt{2}g}=m^{-1}$.

2. Non-SUSY AdS_6 vacuum: $X=3^{-1/4}$

The nonsupersymmetric AdS_6 vacuum of Romans supergravity is defined by $X=3^{-1/4}$. The geometry of this vacuum takes the following form:

$$\begin{aligned} ds_{10}^2 &= s^{-1/3}[(3-2c^2)^{1/2}ds_{\mathrm{AdS}_6}^2 + 2g^{-2}3^{-1/2}(3-2c^2)^{1/2}d\xi^2 \\ &\quad + 2g^{-2}3^{1/2}(3-2c^2)^{-1/2}c^2 d_{S^3}^2], \\ e^{\Phi} &= 3^{1/4}s^{-5/6}(3-2c^2)^{1/4}, \\ F_{(4)} &= 12\sqrt{2}g^{-3}(3-2c^2)^{-2}s^{1/3}c^3 d\xi\wedge \mathrm{vol}_{S^3}, \end{aligned} \tag{35}$$

with the radius of AdS_6 given by $L_{\mathrm{SU/SY}}=\frac{3^{1/4}5^{1/2}}{2^{1/2}g}=\frac{\sqrt{5}}{3^{3/4}m}$. As for the nonsupersymmetric AdS_7 (12), the brane origin of this vacuum is not clear.

B. First-order formulation for dS_5 domain walls

Let us focus on domain wall geometries of the following form:

$$\begin{aligned} ds_6^2 &= e^{2A(r)}L^2 ds_{\mathrm{dS}_5}^2 + dr^2, \\ X &= X(r). \end{aligned} \tag{36}$$

The equations of motion (33) take the form of two ODEs and the Hamiltonian constraint,

$$\begin{aligned} A'' + 5A'^2 - \frac{4e^{-2A}}{L^2} + \frac{1}{4}V = 0, \\ X'' + 5A'X' - \frac{X'^2}{X^2} - \frac{1}{8}X^2\partial_X V = 0, \\ 20A'^2 + \frac{4X'^2}{X^2} - \frac{20e^{-2A}}{L^2} + V = 0, \end{aligned} \tag{37}$$

where the derivative with respect to r has been denoted by $'$. The geometry of AdS_6 vacua can be recovered by choosing

[7]More precisely the internal manifold is the upper hemisphere of an S^4 written as a foliation of S^3 over a segment parametrized by the coordinate ξ.

$$A = \log\left(\sinh\left(\frac{r}{L}\right)\right) \tag{38}$$

and imposing $X = 1$ and $L_{\rm SUSY} = m^{-1}$ or $X = 3^{-1/4}$ and $L_{\rm SU/SY} = \frac{\sqrt{5}}{3^{3/4}m}$, respectively, for supersymmetric and non-supersymmetric vacua discussed in the previous section.

Let us construct the quantities needed in order to cast the second-order problem (37) in a system of first-order ODEs. We can follow the same strategy of Sec. III B and outlined in general in the Appendix. It is easy to show that the second-order equations for A and X written in (37) can be obtained by taking the variation of the following 1D effective Lagrangian:

$$L_{\rm eff} = 20e^{5A}A'^2 - 4e^{5A}\frac{X'^2}{X^2} + \frac{20e^{3A}}{L^2} - e^{5A}V. \tag{39}$$

From the expression (A2) we can derive the conjugate momenta $\pi_A = 40e^{5A}A'$ and $\pi_X = -8e^{5A}X^{-2}X'$. Taking the Legendre transformation of (39) we easily obtain the corresponding Hamiltonian

$$H_{\rm eff} = \frac{1}{80}e^{-5A}\pi_A^2 - \frac{1}{16}e^{-5A}X^2\pi_X^2 - \frac{20e^{3A}}{L^2} + e^{5A}V. \tag{40}$$

We are now ready to write the Hamilton-Jacobi equation for the superpotential $F = F(A, X)$ associated with the system (37). By expressing the momenta as $\pi_A = \partial_A F$ and $\pi_X = \partial_X F$, one obtains

$$\frac{1}{80}e^{-5A}(\partial_A F)^2 - \frac{1}{16}e^{-5A}X^2(\partial_X F)^2 - \frac{20e^{3A}}{L^2} + e^{5A}V = 0, \tag{41}$$

where the constant E appearing in (A3) must be zero in order to satisfy the Hamiltonian constraint. As we did in Sec. III B, we reduced the second-order problem (37) to a single PDE. This equation needs to be satisfied by a suitable solution for the superpotential F. Once the solution of the Hamilton-Jacobi equation is found, the radial flow featuring the domain wall (36) can be worked out easily through by integrating the first-order equations (A5). In this specific case, they have the form

$$A' = \frac{1}{40}e^{-5A}\partial_A F \quad \text{and} \quad X' = -\frac{1}{8}e^{-5A}X^2\partial_X F. \tag{42}$$

The solutions of (42) solve automatically also the equations of motion since, as explained in the Appendix, they imply the extremization of the action (39).

C. The interpolating solution

In this section, we will follow the same strategy of numerical integration as in Sec. III C. The idea is to solve perturbatively the Hamilton-Jacobi equation (41) by expanding around the nonsupersymmetric AdS_6 vacuum (35). Let us start by checking the reliability of the perturbative analysis. To this aim, we may compare the profile of the scalar potential $V(X)$ given in (31) with its Taylor expansion $V_{\rm pert}(X)$ around the nonsupersymmetric vacuum $X = 3^{-1/4}$. From Fig. 4, it is manifest that if the perturbative order is sufficiently high then the scalar potential can be substituted by its perturbative expansion in the interval $X \in [3^{-1/4}, 1]$.

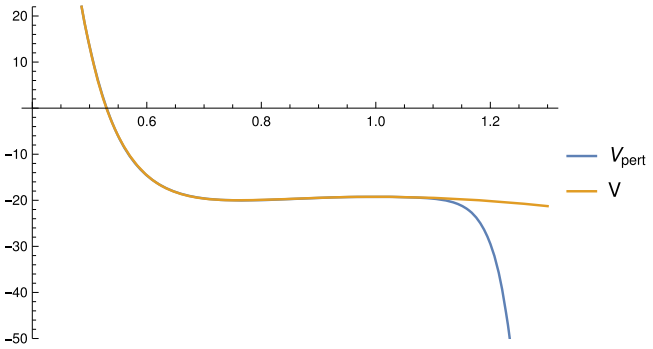

FIG. 4. The comparison between the scalar potential $V(X)$ given in (31) and its expansion at 15th order around the non-SUSY critical point $X = 3^{-1/4} \simeq 0.75$. For values of X between the two critical points $X \in [3^{-1/4}, 1]$, the scalar potential is well approximated by its perturbative expansion. The plot is given for $m = \frac{\sqrt{2}}{3}g = 1$.

In order to solve the Hamilton-Jacobi equation, we need to impose suitable boundary conditions on the derivatives of the fake superpotential. It is easy to verify that the expression

$$F_\infty = \frac{10}{L}e^{4A} - \frac{L}{6}e^{6A}V \tag{43}$$

solves Eq. (41) in small L limit, up to orders $O(L^2)$. The expression F_∞ describes the highly curved regime of small values of L in which the contribution of dS_5 is dominant in the stress-energy tensor. We can use (43) to produce the initial conditions on the derivatives of $F(A, X)$ at each order of the perturbative expansion. Let us recall the ansatz (24) for the fake superpotential expanded around the nonsupersymmetric vacuum,

$$F(A, X) = 4\sum_{k=0}^{\infty} F^{(k)}(A)\frac{(X - 3^{-1/4})^k}{k!}, \tag{44}$$

where the coefficients $F^{(k)}$ need to depend on A to take into account the nonseparability of the effective potential defining the Hamiltonian (40). With this ansatz, the Hamilton-Jacobi equation (41) becomes a set of ODEs for the coefficients $F^{(k)}(A)$, each for any order in k. As for the 7D case, we impose $F^{(1)}(A) = 0$ in order to keep each perturbative order decoupled. At the zeroth order, one obtains

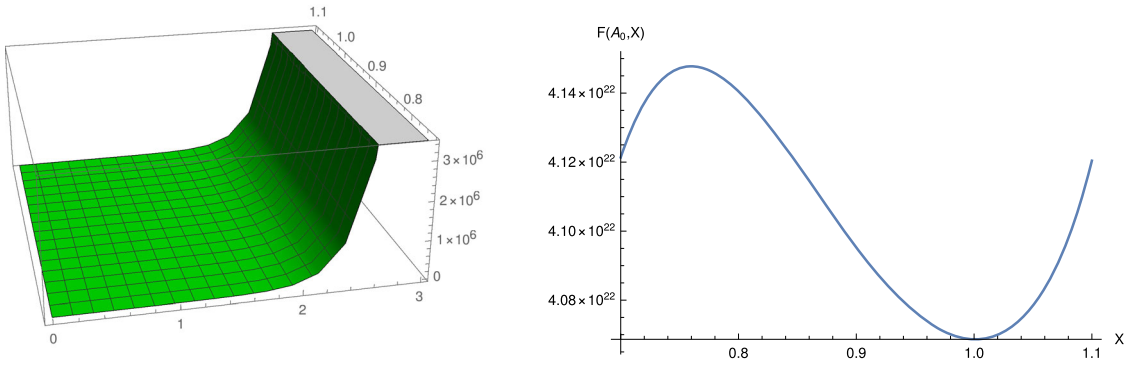

FIG. 5. The profile of the superpotential $F(A, X)$ obtained with perturbative integration up at order $k = 15$. The 3D plot describes the full solution in the intervals $A \in [0, 3]$ and $X \in [0.74, 1.1]$. On the right side, the same function is plotted for $A_0 = 10$. Even if the variation of F is tiny, we observe an interpolating profile between the two AdS_6 vacua, respectively, located at $X = 3^{-1/4} \simeq 0.75$ and $X = 1$. The plots are given for $L = 1$.

$$\frac{1}{5}e^{-5A}(\dot{F}^{(0)})^2 - \frac{20e^{5A}}{L^2} - \frac{20e^{3A}}{L^2} = 0, \tag{45}$$

where the derivative with respect to A has been denoted by $\cdot$ and we expressed the scalar potential in terms of the radius of the non-SUSY vacuum through the relation $m = \frac{3^{3/4}}{\sqrt{5}}L$ characterizing the non-SUSY vacuum (35). This equation can be solved exactly; this procedure leading to an expression similar to (26). After determining the profile of $F^{(2)}(A)$ numerically, one can integrate each ODE belonging to the perturbative tower, finding the coefficients $F^{(k)}(A)$. At each order in $k \geq 2$ the numerical integration one has to evaluate the $(k-1)$th solution of the previous step in the kth ODE for $F^{(k)}(A)$. As we did for the initial conditions (27) for the 7D case, we impose the following boundary conditions:

$$F^{(k)} = 4^{-1}\partial_X^k F_\infty^{(k)}|_{X=3^{-1/4}}, \tag{46}$$

where $F_\infty^{(k)}$ is given by (43) and it has been written in terms of the perturbative expansion of the scalar potential V at the kth order. The solution for $F(A, X)$ obtained by iterating the numerical integrations up to the order $k = 15$ is plotted in Fig. 5. Also in this case we observe an interpolating flow of the superpotential between the two vacua. The last step is integrating the first-order equations (42) using the numerical solution for $F(A, X)$. We perform this radial integration by taking as initial value the nonsupersymmetric vacuum placed at $r = 0$. The result of this integration for A and X is plotted in Fig. 6. We observe that the radial flow of the domain wall smoothly connects the nonsupersymmetric AdS_6 vacuum to the Brandhuber-Oz vacuum of massive IIA.

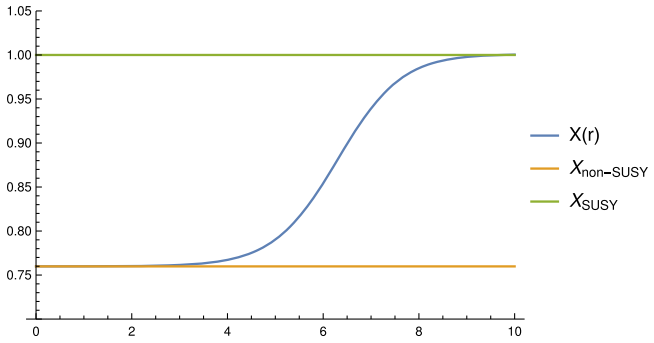

FIG. 6. The smooth radial flows of the scalar X of the dS_5-sliced domain wall in comparison with those of the two AdS_6 vacua.

V. FINAL COMMENTS

In this work, we presented the methodology to provide the geometries describing gravitational instantons connecting two different AdS vacua, one preserving SUSY and the other not. The key feature of our solutions is that they are fully backreacted in the sense that we did not have to make use of probe calculations in order to study a tunneling process, nor have we imposed the thin-wall approximation at the interface between the two vacua.

Nevertheless, there are many features of our solutions that still require a deeper understanding and this paper aims at representing a first intermediate step in this research direction. A quite mysterious element is related to the brane interpretation of our 7D and 6D dS domain walls. Interesting results regarding the microscopic origin of the nonperturbative instability of the non-SUSY AdS vacua considered in this paper have been obtained by looking at the 7D supergravity as a compactification of massive IIA string theory [33,34]. For what concerns the 6D case, in [35] the analysis on the nonperturbative instability of the non-SUSY AdS_6 vacuum has been performed by embedding the Romans supergravity in type IIB. An ambitious step forward would be obtaining the aforementioned non-SUSY vacuum

geometries as the near-horizon regime of a suitable brane solution or, at least, to provide a clear understanding of the microscopic objects underlying their nonperturbative decays in the spirit of the analysis of the (singular) solutions of [36] and, more recently, of [37].

Furthermore, a relevant aspect to investigate is the possibility of applying our solutions to string cosmology. In [38,39], a proposal of dS_4 cosmology was formulated in the context of type IIB starting from the imposition of Israel junction conditions between two AdS_5 vacua, one of which is supersymmetric and the other not. The mechanism identified in the aforementioned references as responsible for the emergence of de Sitter geometry at the interface of the two AdS vacua was exactly the Coleman–de Luccia decay of the vacuum with broken SUSY. With the approach outlined in this paper, it would be interesting to test this proposal by deriving the fully backreacted solution describing this construction in type IIB.

Another interesting issue that seems to require further clarifications and better understanding is the relation of our work to positive energy theorems in string compactifications. Strictly speaking, the existence of our dS domain walls may appear in contradiction to the analysis in [29,30], where the existence of global fake superpotentials bounding the scalar potential from below is argued to be a sufficient condition for vacuum stability. Our present findings seem to restrict the validity of such positive energy theorems in a gauged supergravity to the set of solutions corresponding to a given choice of branch for the superpotential. Other flows associated with different fake superpotentials belong to disconnected subsets of the space of solutions to the Hamilton-Jacobi equations. Because of this, globally bounding superpotentials might, after all, have nothing conclusive to say about nonperturbative (in)stabilities. A decisive analysis one needs to go through in order to assess the contribution of our bubbles to the Euclidean path integral is to extract the effective wall tension and see whether it respects the CdL bound. However, we should also stress that this procedure for thick walls is not free of subtleties and ambiguities. We hope to come back to this issue in the future.

We would like to conclude by reflecting on a final aspect concerning our present results. Back in the original literature from the 1980s, a semiclassical Euclidean path integral approach was used in order to come up with physical predictions for false vacuum decay. We should definitely stress that our 6D and 7D theories arising from consistent truncations of string and M theory can never be regarded as good effective theories in a Wilsonian sense. We only used the truncation formulas as a technique to produce 10D and 11D solutions involving expanding bubbles within AdS. Hence, a proper estimation of the nucleation probability should be directly performed within the higher-dimensional description.

ACKNOWLEDGMENTS

The work of N. P. is supported by the Israel Science Foundation (Grant No. 741/20) and by the German Research Foundation through a German-Israeli Project Cooperation (DIP) Grant "Holography and the Swampland."

APPENDIX: HAMILTON-JACOBI METHOD FOR CLASSICAL SYSTEMS

In this appendix, we schematically review the Hamilton-Jacobi formulation in studying the dynamics classical systems.[8] The power of this method is to allow one to cast the equations of motion of a classical system in terms of a set of first-order constraints, even in the absence of supersymmetry.

The starting idea is to formulate the variational principle for a given configuration by recasting the action into a sum of various squares. Requiring that each of these squares vanish separately determines a set of first-order ODEs. The solutions of these first-order equations solve the equations of motion by construction.

The general form of these first-order conditions can be determined in generality as follows. Let us start by a generic action of the form

$$S(q,r)=\int drL \quad \text{with} \quad L=\frac{1}{2}M_{\alpha\beta}\dot{q}^{\alpha}\dot{q}^{\beta}-V(q). \tag{A1}$$

The "time" parameter has been called r since, for the cases we are interested in, the aforementioned action is obtained by reducting some (super)gravity system to one dimension. Then the 1D time typically describes the radial flow of some (super)gravity solution. The variables $q^{\alpha}(r)$ turn out to describe the dynamical functions associated with the gravity background under study (e.g., the warp factors, scalar fields, etc.). With a Legendre transformation, one can derive the Hamiltonian,

$$H=\frac{1}{2}M^{\alpha\beta}p_{\alpha}p_{\beta}+V(q)\,\text{with}\,p_{\alpha}=\partial_{\dot{q}^{\alpha}}L=M_{\alpha\beta}\dot{q}^{\beta}. \tag{A2}$$

The core of this approach consists of the introduction of a "superpotential" $F(q)$. This function includes all the information to identify the dynamics of the system. The superpotential can be defined through the so-called Hamilton-Jacobi equation,

$$H(\partial_q F,q)+\frac{\partial S}{\partial r}=\frac{1}{2}M^{\alpha\beta}\partial_{\alpha}F\partial_{\beta}F+V-E=0 \quad \text{with} \quad p_{\alpha}=\partial_{\beta}F, \tag{A3}$$

where the action has been crucially interpreted as a function of the dynamical variables with the form $S(q)=F(q)-rE$

[8]See also appendixes of [40] and Ref. [29] for more details.

with E constant. We can now use (A3) to cast the action into a sum of squares. Expressing the potential $V(q)$ in terms of the superpotential by using (A3) and plugging the expression in the action, we get up to total derivatives,

$$S = \frac{1}{2}\int dr M_{\alpha\beta}(\dot{q}^\alpha - M^{\alpha\gamma}\partial_\gamma F)(\dot{q}^\beta - M^{\beta\delta}\partial_\delta F). \quad \text{(A4)}$$

Setting to zero each of these squared produces the following system of ODEs:

$$\dot{q}^\alpha = M^{\alpha\beta}\partial_\beta F. \quad \text{(A5)}$$

By construction, the solutions of the above differential conditions extremize the action. As we mentioned at the beginning of this appendix, this method does not rely on any supersymmetry completion when it is applied on a given supergravity background and, for this reason, it constitutes a good method in searching for nonsupersymmetric solutions characterized by nontrivial radial flows.

[1] A. Strominger and C. Vafa, Microscopic origin of the Bekenstein-Hawking entropy, Phys. Lett. B **379**, 99 (1996).
[2] J. M. Maldacena, The large N limit of superconformal field theories and supergravity, Adv. Theor. Math. Phys. **2**, 231 (1998).
[3] V. Kumar and W. Taylor, String universality in six dimensions, Adv. Theor. Math. Phys. **15**, 325 (2011).
[4] A. Adams, O. DeWolfe, and W. Taylor, String Universality in Ten Dimensions, Phys. Rev. Lett. **105**, 071601 (2010).
[5] C. Vafa, The string landscape and the Swampland, arXiv: hep-th/0509212.
[6] E. Palti, The Swampland: Introduction and review, Fortschr. Phys. **67**, 1900037 (2019).
[7] M. van Beest, J. Calderón-Infante, D. Mirfendereski, and I. Valenzuela, Lectures on the Swampland program in string compactifications, Phys. Rep. **989**, 1 (2022).
[8] N. Arkani-Hamed, L. Motl, A. Nicolis, and C. Vafa, The string landscape, black holes and gravity as the weakest force, J. High Energy Phys. 06 (2007) 060.
[9] E. Witten, Constraints on supersymmetry breaking, Nucl. Phys. **B202**, 253 (1982).
[10] H. Ooguri and C. Vafa, Non-supersymmetric AdS and the Swampland, Adv. Theor. Math. Phys. **21**, 1787 (2017).
[11] D. Harlow, Metastability in anti de Sitter space, arXiv: 1003.5909.
[12] P. Narayan and S. P. Trivedi, On the stability of non-supersymmetric AdS vacua, J. High Energy Phys. 07 (2010) 089.
[13] S. R. Coleman and F. De Luccia, Gravitational effects on and of vacuum decay, Phys. Rev. D **21**, 3305 (1980).
[14] J. D. Brown and C. Teitelboim, Neutralization of the cosmological constant by membrane creation, Nucl. Phys. **B297**, 787 (1988).
[15] K. Skenderis and P. K. Townsend, Hamilton-Jacobi method for curved domain walls and cosmologies, Phys. Rev. D **74**, 125008 (2006).
[16] J. K. Ghosh, E. Kiritsis, F. Nitti, and L. T. Witkowski, Revisiting Coleman–de Luccia transitions in the AdS regime using holography, J. High Energy Phys. 09 (2021) 065.
[17] M. Cvetic, H. Lu, and C. N. Pope, Consistent Kaluza-Klein sphere reductions, Phys. Rev. D **62**, 064028 (2000).
[18] M. Cvetic, H. Lu, and C. N. Pope, Gauged Six-Dimensional Supergravity from Massive Type IIA, Phys. Rev. Lett. **83**, 5226 (1999).
[19] H. Lu and C. N. Pope, Exact embedding of $N = 1$, $D = 7$ gauged supergravity in $D = 11$, Phys. Lett. B **467**, 67 (1999).
[20] M. Cvetic, S. Griffies, and H. H. Soleng, Nonextreme and Ultraextreme Domain Walls and their Global Space-Times, Phys. Rev. Lett. **71**, 670 (1993).
[21] W. Israel, Singular hypersurfaces and thin shells in general relativity, Nuovo Cimento B **44S10**, 1 (1966); **48**, 463(E) (1967).
[22] M. Cvetic, S. Griffies, and S.-J. Rey, Static domain walls in $N = 1$ supergravity, Nucl. Phys. **B381**, 301 (1992).
[23] M. Cvetic, S. Griffies, and S.-J. Rey, Nonperturbative stability of supergravity and superstring vacua, Nucl. Phys. **B389**, 3 (1993).
[24] L. Randall and R. Sundrum, An Alternative to Compactification, Phys. Rev. Lett. **83**, 4690 (1999).
[25] K. Pilch, P. van Nieuwenhuizen, and P. K. Townsend, Compactification of $d = 11$ supergravity on S(4) (or $11 = 7 + 4$, too), Nucl. Phys. **B242**, 377 (1984).
[26] H. Nastase, D. Vaman, and P. van Nieuwenhuizen, Consistent nonlinear K K reduction of 11-d supergravity on AdS (7) x S(4) and self-duality in odd dimensions, Phys. Lett. B **469**, 96 (1999).
[27] P. K. Townsend and P. van Nieuwenhuizen, Gauged seven-dimensional supergravity, Phys. Lett. **125B**, 41 (1983).
[28] M. Cvetic, S. Griffies, and H. H. Soleng, Local and global gravitational aspects of domain wall space-times, Phys. Rev. D **48**, 2613 (1993).
[29] G. Dibitetto, Positive energy and non-SUSY flows in ISO(7) gauged supergravity, Universe **8**, 293 (2022).
[30] U. H. Danielsson, G. Dibitetto, and S. C. Vargas, Universal isolation in the AdS landscape, Phys. Rev. D **94**, 126002 (2016).
[31] L. J. Romans, The F(4) gauged supergravity in six-dimensions, Nucl. Phys. **B269**, 691 (1986).
[32] A. Brandhuber and Y. Oz, The D4—D8 brane system and five-dimensional fixed points, Phys. Lett. B **460**, 307 (1999).

[33] F. Apruzzi, G. Dibitetto, and L. Tizzano, A new 6d fixed point from holography, J. High Energy Phys. 11 (2016) 126.
[34] F. Apruzzi, G. Bruno De Luca, A. Gnecchi, G. Lo Monaco, and A. Tomasiello, On AdS_7 stability, J. High Energy Phys. 07 (2020) 033.
[35] F. Apruzzi, G. Bruno De Luca, G. Lo Monaco, and C. F. Uhlemann, Non-supersymmetric AdS_6 and the swampland, J. High Energy Phys. 12 (2021) 187.
[36] G. T. Horowitz, J. Orgera, and J. Polchinski, Nonperturbative instability of $AdS_5 \times S^5/\mathbb{Z}_k$, Phys. Rev. D **77**, 024004 (2008).
[37] P. Bomans, D. Cassani, G. Dibitetto, and N. Petri, Bubble instability of mIIA on $AdS_4 \times S^6$, SciPost Phys. **12**, 099 (2022).
[38] S. Banerjee, U. Danielsson, G. Dibitetto, S. Giri, and M. Schillo, Emergent de Sitter Cosmology from Decaying Anti–de Sitter Space, Phys. Rev. Lett. **121**, 261301 (2018).
[39] S. Banerjee, U. Danielsson, G. Dibitetto, S. Giri, and M. Schillo, de Sitter cosmology on an expanding bubble, J. High Energy Phys. 10 (2019) 164.
[40] G. Dibitetto, N. Petri, and M. Schillo, Nothing really matters, J. High Energy Phys. 08 (2020) 040.